An Adaptive Automatic Algorithm for Extracting Geological Lineaments in AL-Dibdibba Formation Basin

Alaa S. Mahdi, Laith A. Jawad*
Remote Sensing Unit, College of Science, Baghdad University, Baghdad, Iraq.

Abstract

Iraq is one of the Arabian area countries, which considered from the drier areas on the earth, though it has two main rivers that pass through(Tigris and Euphrates); it suffers the same problem as them (drought), only the rivers' nearby regions make use of their water for (domestic, agricultural, and industrial purposes).

One of the usable solutions is to utilize the groundwater (especially in the desert regions). Using the Remote Sensing and geographic information system is a rapid and coast effective techniques, they provide information of large and inaccessible area within short span for assessing, monitoring, and management of groundwater resources. In this study, an adaptive algorithm based on Canny edge detector noise reduction idea and directional filters scheme submitted for lineaments automatically extraction from LandSat7 (Enhanced Thematic Mapper Plus) ETM+ band 7 data considering the lineaments spatial and spectral characteristics, yet the algorithm validation examined using ancillary data of the same interest (Iraq tectonic map and 90m SRTM DEM). The analysis process achieved using Arc GIS 9.3 to recognize the potential groundwater renewal and/ or accumulative zones in the selected arid to semi-arid area (AL-Dibdibba formation basin).

Keywords: lineaments, automatically extraction algorithm, groundwater flow, and renewal groundwater.

خوارزمية آلية مطورة لاستخلاص التراكيب الخطية الجيولوجية في حوض تكوين الدبدبة

علاء سعود مهدي و ليث عزيز جواد*.
وحدة الاستشعار عن بعد، كلية العلوم، جامعة بغداد، بغداد، العراق.

الخلاصة

العراق هو أحد البلدان العربية، والتي تعد من أكثر بلدان العالم جفافاً، وعلى الرغم من امتلاكه لنهرين رئيسين يمران من خلاله (دجلة والفرات) فانه يعاني نفس المشكلة (الجفاف). المناطق القريبة من النهرين هي وحدها المستفيدة من مياههما للأغراض (المنزلية، الزراعية، والصناعية).

أحد الحلول القابلة للتطبيق هو استخدام المياه الجوفية (خصوصاً في المناطق الصحراوية). إن الاستشعار عن بعد ونظم المعلومات الجغرافية هي تقنيات سريعة وغير مكلفة، فهما تزودانا بالمعلومات عن مساحات واسعة وغير قابلة للوصول أحيانا بفترة زمنية قصيرة لأجل تقييم، مراقبة، وإدارة مصادر المياه الجوفية.في هذا البحث، تم تقديم خوارزمية مطورة اتخذت من طريقتي(Canny edge detector, directional filters) أساسا لها لاستخلاص التراكيب الخطية آلياً من بيانات الحزمة السابعة لصور القمر الصناعيLandsat7 (راسم الخرائط الموضوعية المعززة) وذلك بأخذ الخصائص المكانية والطيفية للتراكيب الخطية بنظر الاعتبار، بعد ذلك تم اختبار المصداقية العملية لهذه الخوارزمية باستخدام البيانات الملحقة عن

*Email: laithazeez-24@yahoo.com

نفس الموضوع (خارطة العراق التكتونية ونموذج الارتفاعات الرقمي للقمر SRTM بوضوحية موضوعية 90مترا). عمليات التحليل تمت باستخدام برنامج Arc GIS 9.3 لتمييز المناطق الواعدة بوجود المياه الجوفية المتجددة و/ أو المتراكمة في المنطقة الجافة إلى شبه الجافة قيد الدراسة (حوض تكوين الدبدبة).

Introduction:

Geological lineaments extraction and mapping is considered as a very important issue for the hydrogeological research[1], problem solving in engineering, especially, in site selection for construction (dams, bridges, roads, and so on), seismic and landslide risk assessment [2], mineral exploration [3], etc.

Lineaments are the linear, rectilinear, curvilinear features of tectonic origin observed in aerial or satellite data. These lineaments normally show tonal, textural, soil tonal, relief, drainage and vegetation linearity and curvilinearity in satellite imagery [4]. Any linear features that can be picked out as lines (appearing as such or evident because of contrasts in terrain or ground cover on either side) in aerial or space imagery. If geological these are usually faults, joints, or boundaries between stratigraphic formations. Other cause of lineaments include roads and railroads, contrast-emphasized contacts between natural or man-made geographic features (e.g. fence lines), or vague "false alarms" caused by unknown (unspecified) factors [5].

Lineament photointerpretation is a quite subjective process, requires expertise, training, scientific skills and is time consuming and expensive. Therefore, the need arises for automation of photointerpretation in order to reduce subjectivity and help the analysts [6].

The main objective of this study is to propose an algorithm that automatically extract geological lineaments form the aerial or space imagery data, then examine its validity using ancillary data of the same interest (tectonic map and relief DEM), another objective is to analyze these lineaments for groundwater (follow and potential zones) identification.

The Study Area

The study area is AL-Dibdibba formation basin, which falls in the middle part of Iraq, it comprises of districts from four administratives (Karbala, Najaf, Babil, and Anbar). Its borders identified by applying the 3D analyst tools in Arc GIS 9.3 (interpolate line and create profile graph) on the 90m SRTM elevation model to recognize the recharging and discharging zones of the basin. The basin extends between the latitudes 31º 54´ N and 32º 42´ N and longitudes 43º 38´ E and 44º 33´ E and covers an area of 2706.876 km². The region is arid to semiarid with rare rain storms around the year; the surface water is absent, therefore, rainfall recharged groundwater is very important for the drinking, grazing, and agricultural purposes.

Methodology

The applied methodology is divided into three stages:

1. geodata acquisition and preprocessing
2. lineaments automatically extraction algorithm designing and implementation
3. the validation of the extraction algorithm

Geodata acquisition and preprocessing

In this study two kinds of data were used, the major kind, which is LandSat7 (Enhanced Thematic Mapper Plus) band 7 data, because of its wavelengths that lay between (2.09 µm to 2.35 µm), the matter that make this band a haze free and non affective by the presence of the vegetation (i.e. so preferable for the geological structures detection) [7], also the appropriate spatial resolution (28.5m) and the easy of access to these data. The ancillary kind, which is the relief (Shuttle Radar Topography Mission) Digital Elevation Model with 90m and 30m resolution and the faults map of the study area in order to view the lineaments in their real environment and to evaluate the validity of them (i.e. the faults, joints, and folds must have lineaments that associated with or else the extraction method is not valid) The satellite images of B7 in the path (168_169), row (37_38) that captured at 2001 were

selected and individually enhanced using (background removal and contrast linear stretching) and gathered to make a mosaic one, then extracted to cover the interest area as illustrated in figure-1.

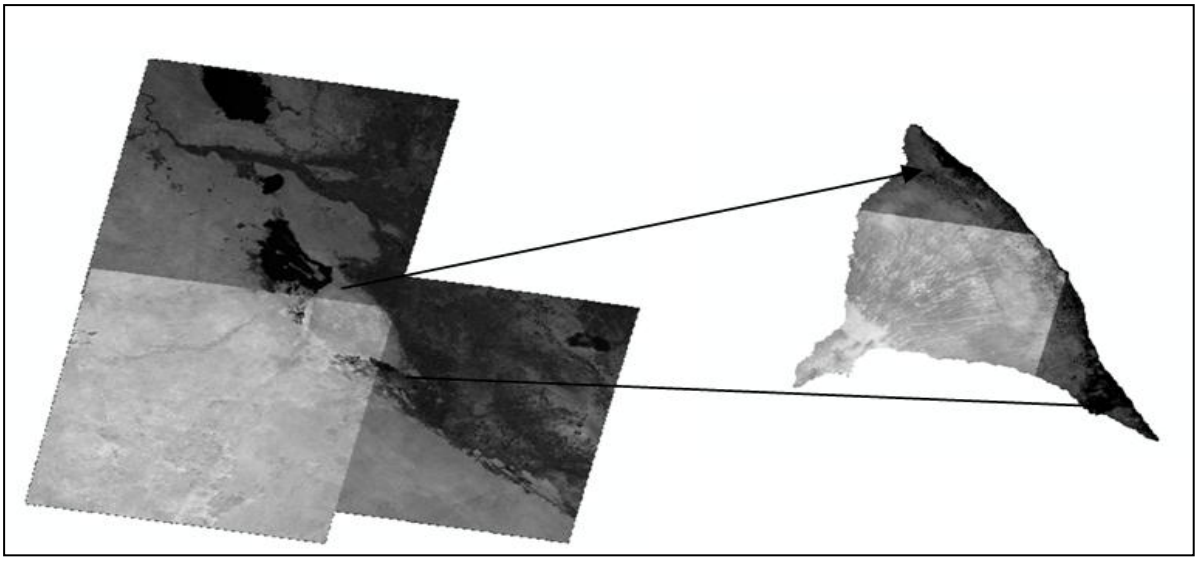

Figure 1- ETM+ band 7 mosaic images comprises the interest area and surroundings and the extracted basin.

3.1Lineaments automatically extraction algorithm designing and implementation

In order to design an algorithm that automatically extract lineaments, lineaments spatial and spectral characteristics should be considered. From the spatial perspective they are straight lines, and highly contrasted structures (with the surrounding environment) from the spectral one.

Adopting these characteristics, the goal is achieved by utilizing edge detector that is not affected by noise and by the same time produces edges in specific orientations. Canny edge detector demonstrate the first demand, but the edges are connected [8], while directional filters such as(Sobel, Perwitt, and Robert) demonstrate the second one, but the influence of the noise is obvious [9] (i.e. the use of each individually is not proper for lineaments extraction).

In this study a new approach is adopted by designing an edge detector that achieves the both aims (noise reduction and oriented edges detection). In the submitted algorithm, Noise reduction was achieved using the (3*3) arithmetic mean filter instead of using the Canny filter formula and the oriented edges detection has been done using the (3*3) directional filters as can be shown in figure-2.

$$\begin{bmatrix} 1 & 0 & -1 \\ 2 & 0 & -2 \\ 1 & 0 & -1 \end{bmatrix} \quad \begin{bmatrix} -1 & 0 & 1 \\ -2 & 0 & 2 \\ -1 & 0 & 1 \end{bmatrix} \quad \begin{bmatrix} -1 & -2 & -1 \\ 0 & 0 & 0 \\ 1 & 2 & 1 \end{bmatrix}$$

$$\begin{bmatrix} 1 & 2 & 1 \\ 0 & 0 & 0 \\ -1 & -2 & 1- \end{bmatrix} \quad \begin{bmatrix} 0 & -1 & -2 \\ 1 & 0 & -1 \\ 2 & 1 & 0 \end{bmatrix} \quad \begin{bmatrix} -2 & -1 & 0 \\ -1 & 0 & 1 \\ 0 & 1 & 2 \end{bmatrix}$$

Figure 2- the (3*3) directional filters in the (N, S, E, W, SE - NW, and SW - NE) respectively.

The Geological lineaments extraction Algorithm:

Step 1: Input a mosaic image of the ETM+ that involves AL-Dibdibba formation basin and its surroundings areas.
Step 2: Reduce the image noise using 3*3 (none weighted) mean filter mask.
Step 3: delineate the oriented edges in the North direction using the (3*3) directional filter matrix with the suitable threshold:

$$\begin{bmatrix} 1 & 0 & -1 \\ 2 & 0 & -2 \\ 1 & 0 & -1 \end{bmatrix}$$

Step 4: saving the resultant binary image (the fracture traces are white and the other contents are black).
Step 5: Go to Step 3
Step 6: delineate the oriented edges in the South direction using the (3*3) directional filter matrix with the suitable threshold:

$$\begin{bmatrix} -1 & 0 & 1 \\ -2 & 0 & 2 \\ -1 & 0 & 1 \end{bmatrix}$$

Step 7: saving the resultant binary image.
Step 8: Go to Step 3
Step 9: delineate the oriented edges in the East direction using the (3*3) directional filter matrix with the suitable threshold:

$$\begin{bmatrix} -1 & 0 & 1 \\ -2 & 0 & 2 \\ -1 & 0 & 1 \end{bmatrix}$$

Step 10: saving the resultant binary image.
Step 11: Go to Step 3
Step 12: delineate the oriented edges in the West direction using the (3*3) directional filter matrix with the suitable threshold:

$$\begin{bmatrix} -1 & -2 & -1 \\ 0 & 0 & 0 \\ 1 & 2 & 1 \end{bmatrix}$$

Step 13: saving the resultant binary image.
Step 14: Go to Step 3
Step 15: delineate the oriented edges in the SW-NE direction using the (3*3) directional filter matrix with the suitable threshold:

$$\begin{bmatrix} 0 & -1 & -2 \\ 1 & 0 & -1 \\ 2 & 1 & 0 \end{bmatrix}$$

Step 16: saving the resultant binary image.
Step 17: Go to Step 3
Step 18: delineate the oriented edges in the NW-SE direction using the (3*3) directional filter matrix

with the suitable threshold:

$$\begin{bmatrix} -2 & -1 & 0 \\ -1 & 0 & 1 \\ 0 & 1 & 2 \end{bmatrix}$$

Step 19: saving the resultant binary image.

The algorithm was implemented using Mat lab 7.0. The lineaments images with six directions exported then to Arc GIS 9.3 to be georeferenced and to make six polylines shape files (the roads, oil pipes, and other artificial straight structures were excluded) then merged to make a final shape file that contains the (non overlapping lineaments) in one theme as illustrated in figure-3.

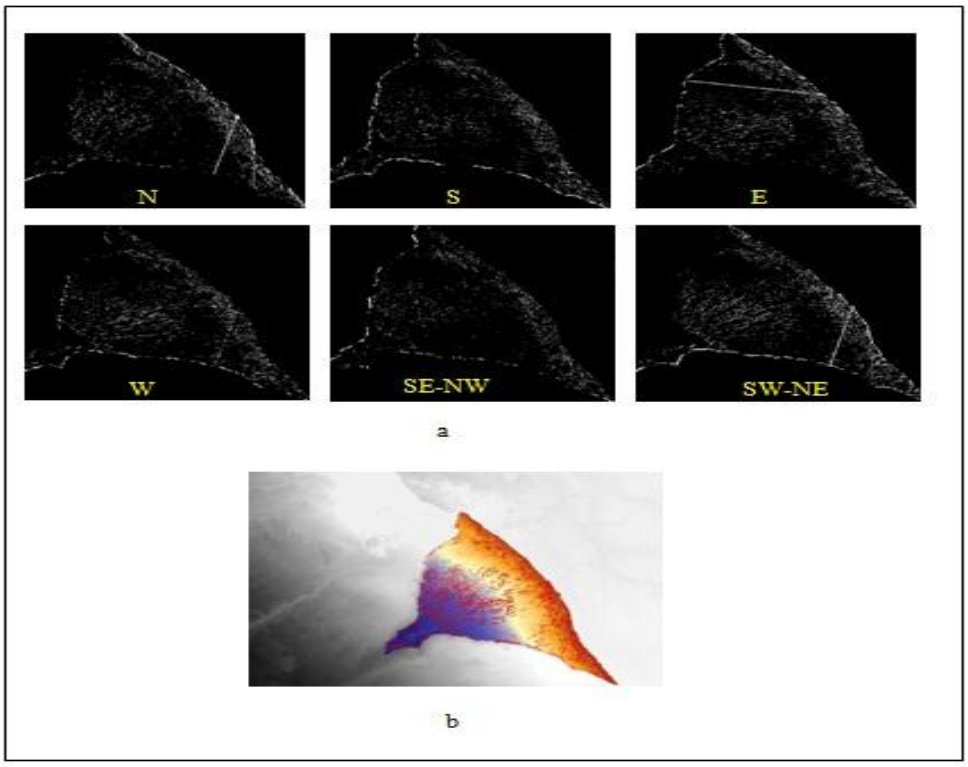

Figure 3- (a) The extracted lineaments images with six orientations (b) The final theme that contains the non overlapping lineaments and their natural appearance on 30m DEM.

3.3 The validation of the extraction algorithm

In order to examine the validity of extracted lineaments, ancillary data utilized, which are the faults map of Iraq and the relief 90m resolution SRTM DEM as illustrated in figure-4, since faults have their associating lineaments with the same extension, which have tonal and height differences with their surrounding, so that the successful algorithm should produce lineaments that spatially obey some of the measured faults. The submitted algorithm interestingly achieved this aim; in addition to that it's capable of small fracture traces extraction, the lineaments number is 2570, which can be reduced by connecting the same orientation spaced ones [10], with lengths in between 77m to 5790m.

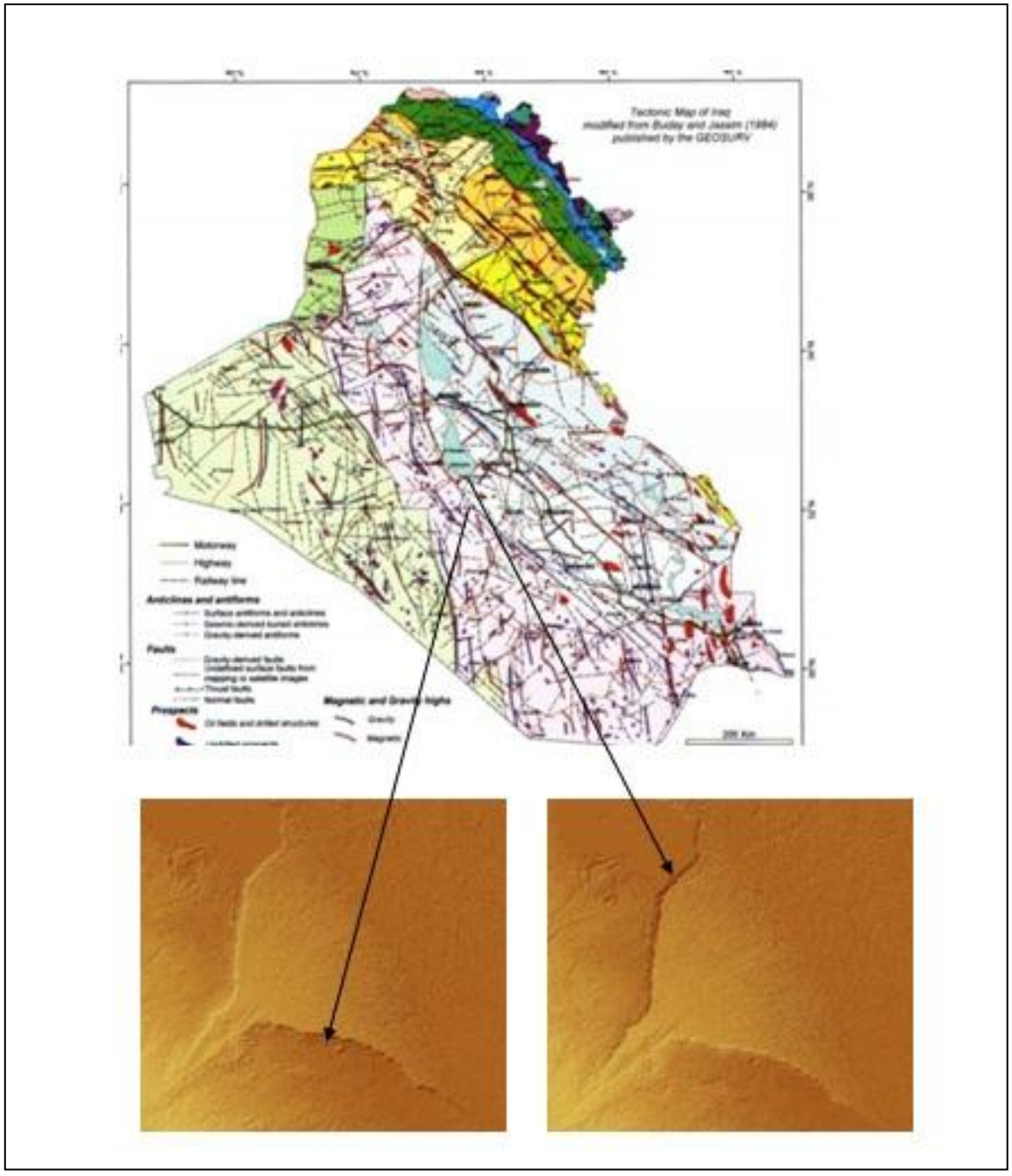

Figure 4- The interest region faults in Iraq tectonic map that appear distinctly in (relief DEM and lineaments final theme).

4. Rustles Analysis

For the analyzing purpose, the interest area was partitioned into a grid of (2 km*2 km) squares, and then the lineaments' longitudes and intersections for each square were measured, summed, and coordinated in the center of the square as illustrated in figure-5.

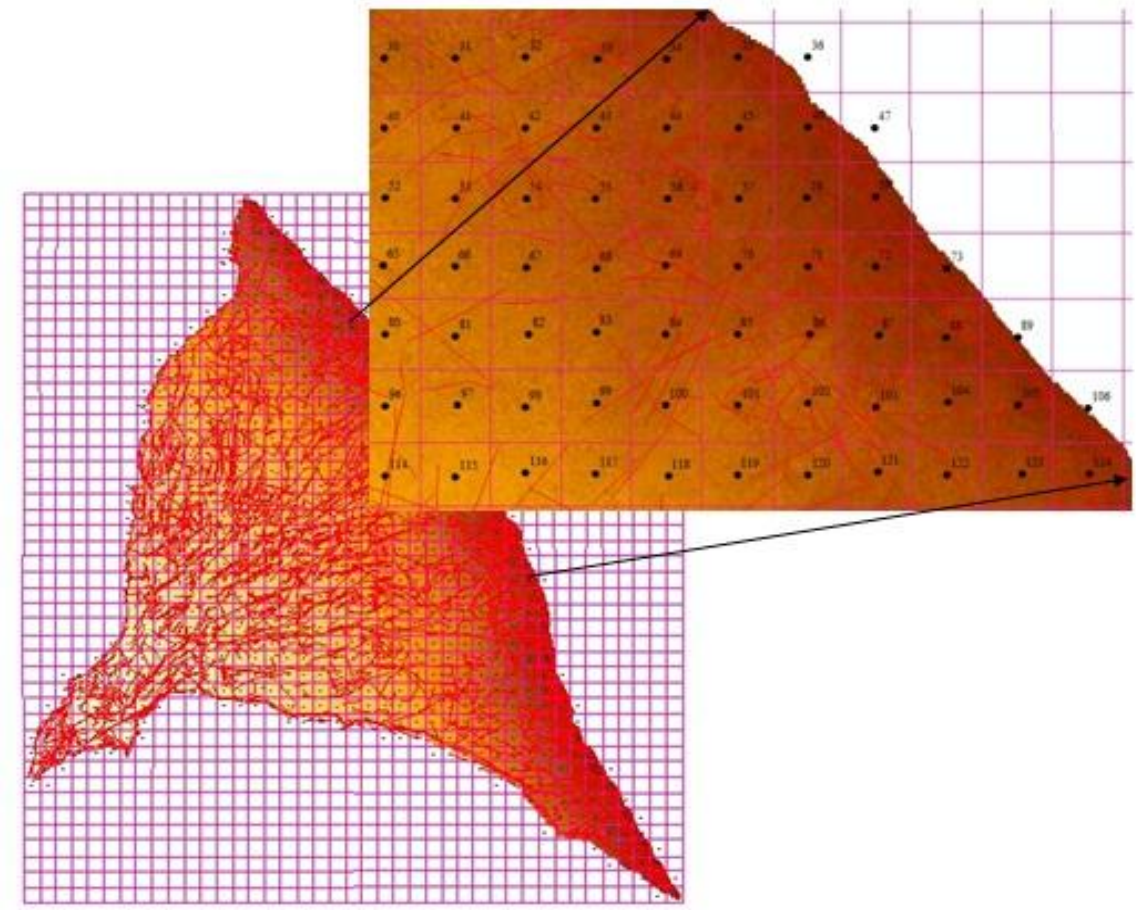

Figure 5- interest area partitioning into a grid of (2 km*2 km) squares with the lineaments longitudinal and intersection density coordinated in each square center.

Two point shape files were created (one for the lineaments longitudinal density and the other for lineaments intersection density). Some interpolation schemes (Kriging, Inverse Distance Weighted, and Natural Neighborhood) were utilized to produce lineaments longitudinal and intersections density distribution maps, these maps are of an optimum importance to discriminate the crust weakest zones, such zones govern the assembling of groundwater and minerals. In figure (6) lineaments longitudinal and intersection density distribution maps interpolated by (IDW, Kriging, and Natural neighborhood) schemes successively and the resultant (intersections, longitudinal) maximum density positions themes and their union one respectively were delineated.

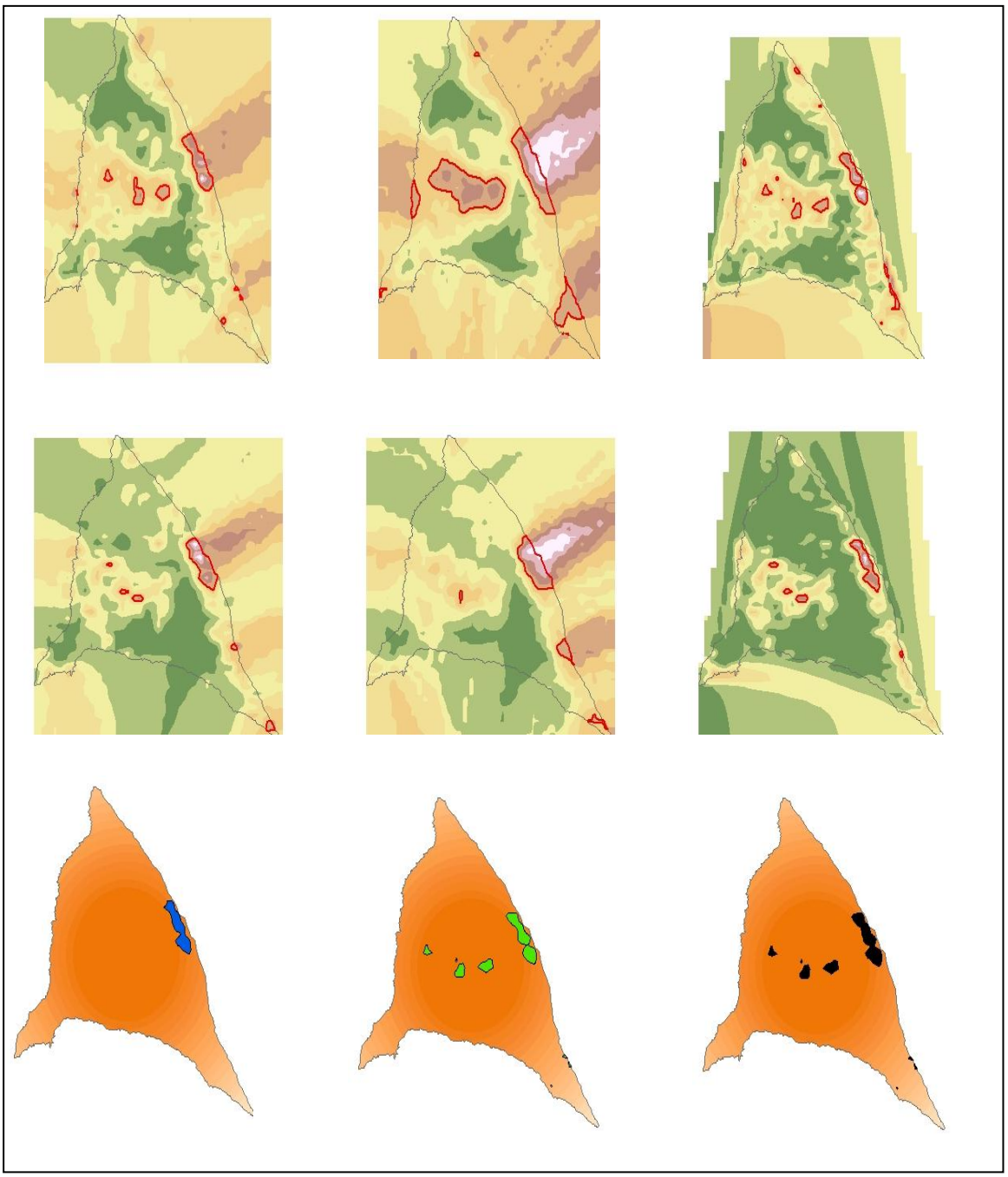

Figure 6- (a) lineaments longitudinal density distribution maps interpolated by (IDW, Kriging, and Natural neighborhood) schemes successively. The maximum longitudinal density of each enclosed by red contour. (b) lineaments intersections density distribution maps interpolated by (IDW, Kriging, and Natural neighborhood) schemes successively. The maximum intersections density of each enclosed by red contours. (c)the resultant (intersections, longitudinal) maximum density positions themes and their union one respectively.

It can be noticed that the maximum density (longitudinal and intersectional) positions to be or become unlike for the three interpolations schemes, so that only the positions that are matching in all of them will be accounted, then the weakest zones can be distinguished by assembling the intersections and longitudinal maximum density positions.

The numerical (frequency) rose diagram were created using (Rock Work 14) to discriminate the major orientations of the lineaments, such ones govern the movement of the groundwater and minerals in the region as can be delineated in figure-7.

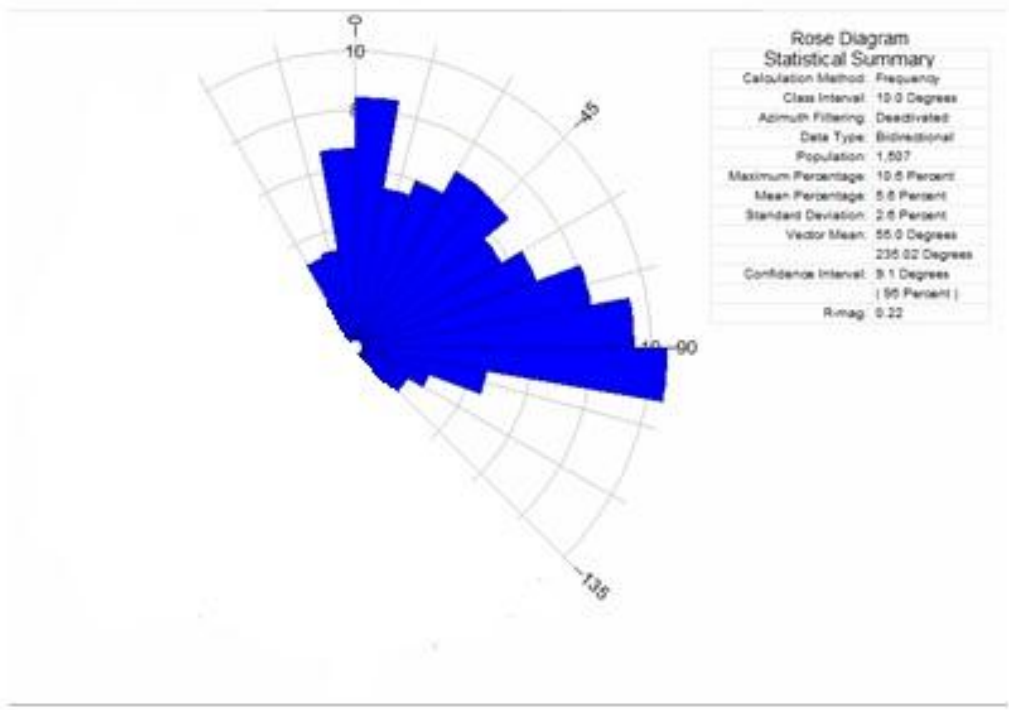

Figure 7- the frequency rose diagram illustrating that the major orientation of the basin lineaments is SW to NE

References

1. Suzen, M.L. and Toprak, V.. **1998**. Filtering of satellite images in geological lineaments analysis: an application to fault zone in Central Turkey, *Int.J. Of remote sensing*, 19, pp:1101-1114.
2. Stefouli, M., Angellopoulos, A. Perantonis, S., Vassilas, N., Ambazis, N. and Charou, E. **1996**. Integrated Analysis and Use of Remotely Sensed Data for the Sesmic Risk assessment of the southwest Peloponessus Greece, First Conference of the Balkan Geophysical Society, Athens Greece, September, pp: 23-27.
3. Tripathi, N. K., Gokhale, K. V. G. K. and Siddiqiqu, M. U. **2000**. Directional morphological image transforms for lineaments extraction from remotely sensed images, *Int.J. of remote sensing*, 21, pp: 3281-3292.
4. Masuda, Sh., Tokuo, T., Ichinosi, Otani, K. and Uchi, T. **1991**. Expert system for lineament extraction from Optical Sensor Data, 2, pp: 10-12.
5. Semere, S., Ghebread, W. **2006**. Lineament characterization and their tectonic significance using landsat TM data and field studies in the central highlands of Eritrea, *Journal of African Earth Science*, 46, pp: 315-318.
6. Demetre, A., Ourania, M., and Marianthi, S. **2000**. Aotumatic mapping of tectonic lineaments (faults) using methods and techniques of Photointerpretation / Digital Remote Sensing and Expert Systems.
7. Lillesand, T.M., Keifer, R.W. **1999**. *Remote Sensing and Image Interpretation*, 4th Edition, pp:312-346.
8. Canny,j.F. **1986**. A computational approach to edge detection, *IEEE trans. On Pat. Anal. And Mach. Int*., 8, pp: 679-714.
9. Meer,P. and Georgesco, B. **1995**. Edge Detection with embedded confidence, *IEEE Trans. On Pat. Anal. And Mach. Int.*, 17, pp: 312-345.
10. Drury, S. **2001**. *Image interpretation in geology*, Blackwell Sciences Inc., pp: 156-163.